AD-A141 859 DEMONSTRATION OF SQUID PARAMETRIC AMPLIFIER(U) TRW SPACE AND TECHNOLOGY GROUP REDONDO BEACH CA ADVANCED PRODUCTS LAB A H SILVER ET AL. 15 MAY 84 1/1

UNCLASSIFIED N00014-81-C-2495 F/G 9/5 NL

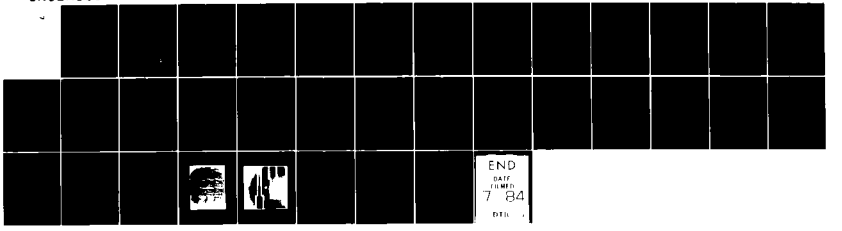

END
DATE FILMED
7 84
DTIC

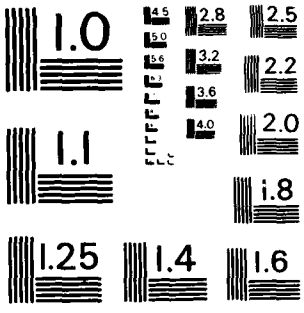

TRW

INTERIM REPORT

DEMONSTRATION OF SQUID PARAMETRIC AMPLIFIER

CONTRACT NO. N00014-81-C-2495
1 OCTOBER, 1983 - 15 MARCH, 1984

Prepared For

THE NAVAL RESEARCH LABORATORY
Code 6854
4555 Overlook Ave., S.W.
Washington, DC 20375

Prepared By

Arnold H. Silver
Robert D. Sandell
Richard R. Phillips
Andrew D. Smith
Advanced Products Laboratory
Applied Technology Division

TRW Space and Technology Group
One Space Park
Redondo Beach, CA 90278

May 15, 1984

INTERIM REPORT

DEMONSTRATION OF SQUID PARAMETRIC AMPLIFIER

CONTRACT NO. N00014-81-C-2495
1 OCTOBER, 1983 - 15 MARCH, 1984

Prepared For

THE NAVAL RESEARCH LABORATORY
Code 6854
4555 Overlook Ave., S.W.
Washington, DC 20375

Prepared By

Arnold H. Silver
Robert D. Sandell
Richard R. Phillips
Andrew D. Smith
Advanced Products Laboratory
Applied Technology Division

TRW Space and Technology Group
One Space Park
Redondo Beach, CA 90278

May 15, 1984

UNCLASSIFIED

SECURITY CLASSIFICATION OF THIS PAGE (When Data Entered)

REPORT DOCUMENTATION PAGE	READ INSTRUCTIONS BEFORE COMPLETING FORM
1. REPORT NUMBER	2. GOVT ACCESSION NO. AD-A141859	3. RECIPIENT'S CATALOG NUMBER
4. TITLE (and Subtitle) Demonstration of SQUID Parametric Amplifier	5. TYPE OF REPORT & PERIOD COVERED Interim Report Oct. 1982 to Mar. 1984
	6. PERFORMING ORG. REPORT NUMBER
7. AUTHOR(s) A. H. Silver, R. D. Sandell, R. R. Phillips, and A. D. Smith	8. CONTRACT OR GRANT NUMBER(s) N00014-81-C-2495
9. PERFORMING ORGANIZATION NAME AND ADDRESS Advanced Products Laboratory TRW Space and Technology Group One Space Park, Redondo Beach, CA 90278	10. PROGRAM ELEMENT, PROJECT, TASK AREA & WORK UNIT NUMBERS P.E. 62762N XF 62-584-004
11. CONTROLLING OFFICE NAME AND ADDRESS Naval Research Laboratory, Code 6854 4555 Overlook Avenue SW Washington DC 20375	12. REPORT DATE May 15, 1984
	13. NUMBER OF PAGES 30
14. MONITORING AGENCY NAME & ADDRESS(if different from Controlling Office)	15. SECURITY CLASS. (of this report) Unclassified
	15a. DECLASSIFICATION/DOWNGRADING SCHEDULE N/A

16. DISTRIBUTION STATEMENT (of this Report)

Approved for Public Release
Unlimited Distribution

17. DISTRIBUTION STATEMENT (of the abstract entered in Block 20, if different from Report)

18. SUPPLEMENTARY NOTES

19. KEY WORDS (Continue on reverse side if necessary and identify by block number)

Parametric amplifier, low noise amplifier, microwave amplifier, Josephson junction, SQUID, array, noise temperature.

20. ABSTRACT (Continue on reverse side if necessary and identify by block number)

TRW has been developing low noise microwave parametric amplifiers with Josephson junction SQUIDs (Superconducting QUantum Interference Devices). This report summarizes the second phase of the program which includes measurement of the amplifier performance at X-band, and design and fabrication of a SQUID array amplifier. We have demonstrated gain in excess of 10 dB at 8.4 GHz and a measured noise temperature equal to 6 K with an uncertainty of (+15/-7)K. Arrays with both 25 and 50 elements and 50 Ω impedance have

DD FORM 1 JAN 73 1473 EDITION OF 1 NOV 65 IS OBSOLETE

UNCLASSIFIED

SECURITY CLASSIFICATION OF THIS PAGE (When Data Entered)

20. continued

been designed and fabricated. These arrays should increase the dynamic range of the amplifier.

1. INTRODUCTION

1.1 Summary

Superconductive electronics incorporating Josephson junctions and SQUIDs (Superconducting QUantum Interference Devices) offers electronic systems of unrivaled sensitivity, speed, and efficiency which are important for the Navy and other DoD agencies. TRW has been developing low noise microwave parametric amplifiers with Josephson junction SQUIDs under Contract No. N00014-81-C-2495 with the Naval Research Laboratory. TRW has demonstrated a nearly degenerate, single idler, parametric amplifier which uses the nonlinear inductance of a single Josephson junction SQUID to provide ultra-low noise amplification. This research has demonstrated 10 dB gain at X-band with measured noise temperature equal to 6K within an uncertainty of (+15 and -7)K. We have also designed and fabricated both 25 and 50 element SQUID arrays which should increase the impedance, saturation power, and dynamic range of the microwave amplifier.

1.2 Objective

The objectives of this project were to provide quantitative measurements of the performance of a low noise SQUID parametric amplifier with respect to gain, noise temperature, bandwidth, and saturation power, and to design and fabricate a SQUID array suitable for use as a higher power low noise amplifier.

1.3 General Background

TRW has been developing low noise SQUID parametric amplifiers based on the design of Silver, et al[1,2] under NRL Contract No. N00014-81-C-2495 since 1981. This unique concept is based on the non-linear inductance of a Josephson junction imbedded in a low $\beta \leq 1$ SQUID, where

$$\beta = 2\pi L i_c / \Phi_o .$$

This design is intended to insure the stability of the junction phase and hence provide ultra-low noise operation, high signal power, and an extension to a stable array configuration with increased dynamic range. TRW has carried out analyses, design, fabrication, and measurements of the single SQUID parametric amplifier at X-band, and designed and fabricated SQUID array amplifiers for X-band experiments.

Parametric amplifier experiments carried out under this contract used a low inductance single junction SQUID connected to a monolithic wideband transformer which couples the 1 Ω stripline SQUID to a 50 Ω coplanar line, and from there to coax via an OSM connector[3]. The pump current is injected via a separate 50 Ω coplanar line. Damping of the SQUID resonance circuit (consisting of the SQUID inductance and the junction capacitance) is by the internal junction quasiparticle conductance and the receiver load.

2. MICROWAVE EXPERIMENTS

2.1 Microwave Probe

The previous experiments[3] were carried out with a waveguide probe and cooled waveguide circulator in a large glass dewar. The circulator magnet was driven by a 500 mA current which produced a large disturbing magnetic field at the device. In addition, the large thermal heat capacity of the waveguide assembly required long turn-around time for experiments.

Early in this phase of the Contract, we decided to change to a more compact coaxial system with a cooled coaxial circulator. The experiments were transferred to the 28 liter helium dewar supplied to TRW by NRL. Coolable X-band coaxial circulators were obtained from P&H Labs., and a new probe assembly was constructed. The new probe used semi-rigid stainless steel coaxial lines with a coaxial circulator in LHe. All dc lines into the probe were filtered to reduce RFI. All coaxial lines were dc connected at only one point to prevent both ground loops and thermal currents between the cold and warm ends. D.c. blocks were used for all microwave cables. Both the signal and pump lines were decoupled from room temperature noise by 20 or 30 dB attenuators at 4K. The coaxial circulator leakage magnetic field was two orders-of-magnitude smaller than that from the previous waveguide circulator. Also, since the magnetic leakage of the coaxial circulator is from a small permanent magnet rather than from an electromagnet which required 500mA, the magnitude of the audio (60Hz) and rf pickup from this source was essentially eliminated. To further reduce the effect of the circulator stray field, the paramp chip was isolated from the circulator by a 5 cm long coaxial line.

Because of a problem in fabricating SQUIDs with the design value of i_c and hence the SQUID-β, we fabricated a small superconducting coil with a persistent mode switch which we placed around the amplifier chip. The field orientation was parallel to the surface of the substrate and the SQUID inductance. The intent was to control the junction critical current without coupling flux to the SQUID inductance. Of course, the orthogonality of the junction control field and the SQUID inductance is not perfect, so that with the comparatively large field required there is some coupling of the magnet flux and the SQUID. We monitored the field effect by observing the depression of the critical current of the test junctions on the edge of the chip. This permitted us to vary the SQUID-β over a range of values during one experimental run. Because the magnet is operated in the persistent mode, there is no measurable noise from field instability. In fact, the persistent mode magnet probably serves as an additional magnetic shield.

2.2 Microwave Measurements

2.2.1 β control

We operated the parametric amplifier with the higher current density junctions by suppressing the critical current with the magnetic field. In this way, we adjusted the SQUID-β to useful values for measurements of the amplifier. This method appears acceptable for proof-of-concept and quantitative evaluation of the amplifier performance. For single junction amplifiers, it may be adaptable for operational devices with on-chip control current inductors. In the persistent mode, the magnet did not produce any readily observable 60 Hz or other interference. Values of β both greater and less than unity could be achieved, and we

were able to distinguish differences in the device operation.

The action of the magnetic field suppression in a SQUID parametric amplifier can be calculated on the basis of the field dependence of the Josephson inductance. Parametric amplification results from the phase-dependent Josephson inductance of the SQUID given by

$$(L_p/L)^{-1} = (1 + \beta\cos\theta).$$

If a magnetic field is applied to a junction, θ becomes a function of position across the junction. For a small, uniform junction in a uniform magnetic field the parametric inductance becomes

$$(L_p/L)^{-1} = (1 + \beta[\sin(X)/X]\cos\theta_o),$$

where θ_o is the average junction phase, $X = (\pi\Phi/\Phi_o)$, and Φ is the magnetic flux in the junction. For junctions small compared with the Josephson length, the flux in the junction is equal to the applied flux coupled to the junction. The SQUID parametric inductance has the same form as that for the unperturbed junction except that β varies by the familiar Fraunhoffer sin(X)/X factor. For large current suppression such as that used here, we effectively have a magnetic vortex situated on the junction. This causes some peculiar and undesirable effects for such large current suppression factors.

With the single junction SQUIDs required for these amplifiers, there is no independent measurement of the junction critical current. Test junctions on the sides of the chip were monitored as we adjusted the magnetic field to suppress the Josephson current. Therefore, we were not able to quantitatively specify (or measure) the value of the SQUID-β. The values of β were estimated both from the observed amplifier characteristics and from independent measurements of the frequency and control current dependence

of the microwave reflectance as performed and analyzed under Contract No. N00014-81-C-0615 with ONR. That analysis showed that the minimum reflectance occurs at a frequency equal to the small signal resonance frequency of the SQUID circuit. Since the SQUID phase control current varies the circuit inductance, it also varies the resonance frequency over a wide frequency range. By curve fitting the reflectance versus phase control current at several frequencies, it will be possible to measure β, Q, and the transformer mismatch at resonance.

A major part of the load conductance at the junction arises from the low voltage quasiparticle conductance of the junction. This situation results from the much higher conductance of the junction compared with the design value. Although the Josephson current can be suppressed by the magnetic field, the normal conductance probably controls the operating Q. Estimates of the junction zero-voltage resistance are several ohms based on measurements of test junctions on the same chip. From the microwave reflectance measurements, the mismatch resistance ratio at resonance is 1.5. Assuming a perfect transformer, we conclude that the effective shunt impedance is either 1.5 Ω or 0.67 Ω.

2.2.2 Experimental method

Figure 1 shows a block diagram of the experimental arrangement for measuring amplifier performance. A klystron supplied a stable X-band signal to the SQUID through a cooled 30 dB attenuator and circulator. The attenuator reduced room temperature noise by 30 dB, effectively eliminating this wide band "signal". The reflected signal was circulated to a room temperature GaAsFET low noise amplifier before being supplied to a spectrum analyzer for power spectrum measurement. Operation of the SQUID amplifier was controlled by adjusting

the applied pump frequency and power, the SQUID dc phase control current, the junction critical current (i.e., β), and the signal power and frequency. The pump signal was supplied from a second klystron at approximately twice the signal frequency through a cold attenuator and a 50:1 impedance mismatch.

Paramp power gain was measured in a two-step process. First, the input power, line losses, and GaAsFET amplifier gain were calibrated by applying a small fixed input signal to the SQUID. With no applied pump power and zero adjusted phase, the SQUID serves as a nearly perfect reflector of very small signals and is nearly ideal for calibration purposes. After the detected output power level is noted, the pump power is turned on and the dc phase is adjusted for maximum signal. The increase in output power level constitutes the parametric amplifier gain.

Noise temperature measurements were made by recording the corresponding rise in the background noise floor with amplifier gain. Noise level measurements were made difficult by the relatively small noise contribution of the SQUID amplifier compared with the noise of the following "low noise" GaAsFET amplifier. Line losses and amplifier gains from the paramp to the spectrum analyzer were measured component-by-component. A calibration factor for paramp output power relative to observed spectrum analyzer power was obtained. As before, the noise level was determined in a two-step process. The spectrum analyzer was set at a frequency removed from the signal frequency but well within the response bandwidth. Measurements were made with the amplifier off to determine the baseline noise due mainly to the GaAsFET amplifier, and with the amplifier on to determine the SQUID contribution. The difference in noise levels

represents the paramp noise. This was converted to the input noise measurement by dividing by the measured paramp gain and subtracting the known residual blackbody noise in the input channel.

2.2.3 Amplifier response

The amplifier performed qualitatively as expected with variation in β, control current (i.e., average junction phase), and pump power. Also, as expected, the noise appeared to increase with the higher gain developed for $\beta > 1$, and strong subharmonic oscillations and noise floor increases were observed with sufficiently high values of pump power and β. As indicated above, the noise was sufficiently low that it was very difficult to measure at low β and for gain near 10 db.

Figure 2 shows a typical amplifier response as observed on the spectrum analyzer. Referring to Fig. 1, the lower curve is the spectrum analyzer response with a klystron signal of -45 dBm at 8.42 GHz either with no pump signal or with the SQUID phase near 0; the upper curve is the response with the pump power on (+4 dBm measured at the pump klystron in this case) and the SQUID phase adjusted for maximum gain. The signal gain is 10.9 dB and an idler appears at

$$f_i = f_p - f_s$$

with gain relative to the input signal equal to 10.5 dB. In this case the noise floor increased by only $\approx$ 0.2 dB when the amplifier gain is turned on, representing amplification of the background input noise.

The observed power levels were consistent with the proposed model[1,2] of the amplifier. The pump power at the SQUID is difficult to quantify because of the intentionally designed, but uncalibrated, mismatches in the pump feed line. Pump power required for typical 10 dB gain varied over more

than 10 dB for different values of β.

Figure 3 shows the response for a higher β case as a function of the signal power. When the small signal gain is set at 17 dB, the (nearly) symmetric spectrum shows nonlinear increase in the amplified signal and idler as well as the appearance of higher order frequency components at higher power. The shifts in the main signal and idler peaks at high power were the result of frequency drift in the klystrons. Each successive trace represents 5 dB increase in input signal power. Some of the nonharmonic structure results from pickup and subsequent amplification of extraneous rf signals. In Fig. 4 we plot the output signal power as a function of the input power. The 3 dB compression point is $\approx$-80 dBm referred to the output, consistent with the previous estimates[2,3].

Figure 5 shows typical observed bandwidths of the amplifier for both low gain (11 dB) and high gain (22 dB). In the low gain case, the pump subharmonic frequency was equal to the passive circuit resonance (8.42 GHz) and the gain curve was well-behaved with a bandwidth $\approx$ 170 MHz. In the high gain case, parametric oscillations were observed at the pump subharmonic for high values of the pump power. The pump subharmonic frequency was offset by 220 MHz to 8.2 GHz and the response was double peaked. The signal gain maxima occurred when either the signal or idler frequencies were within the circuit resonance. The gain was higher and more sharply peaked when the signal was within the resonance bandwidth. The lower gain case in Fig. 5 represents the conditions for which we measured the smallest noise temperature. This bandwidth is smaller than the $\approx$ 840 MHz bandwidth originally predicted[1]. One explanation is that the amplifier figure-of-merit, $G \times BW^2$, is reduced because β is

considerably <1. Another possibility is that the circuit Q is too large. This cannot be resolved without performing the curve fitting to measure both β and Q.

2.2.4 Noise temperature

Table I shows the measured values of the signal, idler, and baseline noise levels for the parametric amplifier at 8.2 GHz. All power levels are referenced to the spectrum analyzer. A correction of -91.0 dBm is subtracted from the measured values in order to adjust for baseline noise levels. The signal gain was observed to be one greater than the idler gain, as expected for a well-coupled SQUID.

Table 2 shows the analysis of the noise temperature of the amplifier. Turning on the amplifier raised the baseline measured at the SA by -104.3 dBm over the 0.1 MHz SA bandwidth. The observed noise level was corrected for amplifier gain and cable loss, resulting in -116.6 dBm noise level referred to the amplifier output. We calculated a total noise rise of 160K above the unamplified case. The unpumped baseline consists of blackbody radiation of 4.2K from the cold attenuator with an additional 0.3K (300K - 30 dB) leakage through the attenuator. This produced a total estimate of the output noise of 164.5K

The amplifier referenced-to-input noise level was obtained by normalizing the output noise by the signal channel gain, leaving 15K. We attribute 9K of this amount to attenuator and feedthrough noise from the signal and idler channels. The best value of the amplifier input noise temperature T_N was determined to be

$$T_N \text{ (SSB)} = 6K \ (+15/-7)K.$$

for a signal gain = 10.3 dB and idler gain = 10.0 dB. The uncertainty in the noise temperature estimate is largely from uncertainty in the measurement of the baseline noise rise.

In the low noise condition, the pump subharmonic oscillation and baseline noise rise did not appear. In another case with higher β and gain = 17 dB, the measured SSB noise temperature was 34K.

We will have to acquire low noise cooled amplifiers to improve the best noise temperature measurements. Ideally this will consist of a second SQUID paramp stage followed by a cooled low noise GaAsFET amplifier.

TABLE 1

SQUID PARAMP POWER LEVELS AT 8.2 GHZ

	Measured Level (dBm)	Corrected For Baseline Noise
Pumped Signal	-73.9	-74.0
Pumped Idler	-74.2	-74.3
Unpumped Signal	-83.5	-84.3
Pumped Baseline	-90.8	-104.3
Unpumped Baseline	-91.0	--
Signal Gain = 10.3 dB = 10.7		
Idler Gain = 10.0 dB = 10.0		

TABLE 2

NOISE TEMPERATURE ANALYSIS

Noise	-104.3 dBm		
Bandwidth (0.1 MHz)	+10.0		
GaAsFET Amplifier Gain	-26.9		
Warm Cable Loss	+1.7		
Cold Cable Loss	+2.0		
Circulator Loss	+0.9		
Excess Output Noise With Pump	-116.9 dBm/MHz	= 160 K	
Blackbody Level (SSB)		+ 4.5K	
Total Output Noise	-116.5 dBm/MHz	164.5K	
Paramp Gain	-10.3 dB		
	-126.8 dBm/MHz	= 15 K	
Blackbody Level (DSB)		-9 K	
Noise Temperature		6 K	
Noise Uncertainty		(+15/-7) K	

3. SQUID ARRAYS

We completed the design for a new wafer with two different SQUID arrays. The arrays were both designed to match directly into 50 ohm coplanar lines. The array impedance is $NZ_o/2$, where N is the number of SQUIDs and Z_o is the impedance of each SQUID. One array has 25 pairs of 4 Ω SQUIDs (each pair of 4 Ω SQUIDs has a series impedance of 2 Ω). The second array has 50 pairs of 2 Ω SQUIDs. This will eliminate further transformer design and test. Also the arrays have damping resistors across each junction, which accurately reflect the analysis and simulations. We have also reduced the chip size to 1x1 cm by eliminating the rather long taper in the coplanar line size reduction. Our earlier test measurements[3] showed no advantage in using the taper. Reducing the chip size will yield more than twice the number of chips on a given wafer. Reduction of the chip size was also dictated by the available step reduction cameras. The earlier masks with 1 X 2 cm. chips were generated directly at the reticle with no step reduction. Because of the smaller feature size associated with the higher impedance SQUIDs, mask generation directly at the reticle was no longer tractable.

The SQUID array layout was redesigned from that which we previously envisioned and sketched in the earlier proposals. Instead of a planar layout anticipated for the SQUID, we have changed over to the sandwich or bridge SQUID. Adjacent single junction SQUIDs in the array are placed parallel to each other with the junctions at opposite ends. With the SQUIDs placed very closely adjacent to each other, the top and bottom metal films of PbInAu and Nb, respectively, were alternately connected as single metal films (Fig. 6). In

this way there is a minimum number of superconducting layers and the array is very compact with a minimum series inductance between the junctions. The masks were designed directly on the Avera CAD system which we acquired during this period. The masks included a new set of test junctions and other structures which can best reflect the characteristics of the parametric amplifier components. Because of the problems with the junction current density, we have added an extra mask which will define an alternate junction size ≈ 25x smaller than the original area.

The array masks were purchased and a complete fabrication was completed during the period-of-performance. Figure 7 shows the first completed array wafer. Each chip contains two different independent arrays and a coplanar coupling line. The design masks for the low current density junctions were used. Figure 8 is a photograph of one chip with the two array structures.

4.0 FABRICATION

Fabrication of the circuit components, particularly the junction and the superconducting contact of the SQUID inductor to the ground plane, continued to be a problem. We have continued to work in this area on this Contract to meet the design values. In addition, we are developing both junction fabrication facilities and processes under TRW IR&D.

Continued efforts to control the Josephson current density near the design value were largely unsuccessful. We have been able to fabricate high quality junctions by thermal oxidation. These junctions have much higher current densities and required a change in the counter-electrode composition and the order of deposition of the counter-electrode and the PbInAu interconnects.

The fabrication steps for the single SQUID paramp and paramp array were similar. The array has seven masks, including a resistor level, compared to five for the single SQUID device. After sputter-deposition of Nb, it was anodized and patterned by chemical or ion beam etching. This layer served as the ground plane for transmission lines and the base electrode. Next an SiO insulating layer was deposited and patterned by lift-off. This layer defined the junction windows and, together with the anodized Nb_2O_5, served as the microstrip dielectric. The junction barrier (native oxide) was thermally grown at 70C after argon ion cleaning; a PbIn counter-electrode was deposited immediately afterward. After an in-situ argon rf plasma cleaning, a PbInAu film was deposited to make superconducting contacts to the counter-electrode and the Nb ground plane in order to form the SQUID inductances. This layer also serves as the transmision lines and connection to the resistors.

Resistors were made with a Au-In compound. In the future, we plan to use more robust materials such as Ti-Au. The PbInAu inter-connect layer will also be replaced by a Nb lift-off layer.

5. PUBLICATIONS

We have submitted the abstract

"Low Noise SQUID Parametric Amplifier"

to the 1984 Applied Superconductivity Conference. A copy is attached as Appendix 1. If accepted, we plan to present this paper at the conference and submit a written manuscript for the Conference Proceedings.

The paper "SQUID Parametric Amplifier" prepared during the previous period-of-performance of this Contract was published in the IEEE Transactions on Magnetics, Vol. MAG-19, pp.622-624 (1983).

6. REFERENCES

1. A. H. Silver, D. C. Pridmore-Brown, R. D. Sandell, and J. P. hurrell, "Parametric Properties of SQUID Lattice Arrays", IEEE Trans. Magn. MAG-17, pp. 412-415 (1981).

2. A. H. Silver, R. D. Sandell, J. P. Hurrell, and D. C. Pridmore-Brown, "SQUID Parametric Amplifier", IEEE Trans. Magn. MAG-19, pp. 622-624 (1983).

3. A. H. Silver, "Demonstration of SQUID Parametric Amplifier", Annual Progress Report, Contract No. N00014-81-c-2495, November, 1982.

7. FIGURES

Figure 1. Block diagram of the microwave experimental arrangement for measuring the SQUID parametric amplifier performance.

Figure 2. Typical small signal amplifier spectral response as recorded from the spectrum analyzer.

Figure 3. High gain spectral response of the SQUID amplifier as a function of signal power. Successive curves were recorded for 5 dB increases in the signal.

Figure 4. Measured output power versus the input power for the signal and intermodulation product as shown in Fig. 3.

Figure 5. Measured spectral response of the SQUID parametric amplifier as a function of signal frequency for both a high gain and low gain case. The pump subharmonic frequency is shown by the arrows on the graph.

Figure 6. Schematic drawing of the geometry of the SQUID paramp array (not to scale).

Figure 7. Photograph of a fabricated paramp array two inch silicon wafer.

Figure 8. Photograph of the SQUID paramp array chip showing the two different size arrays.

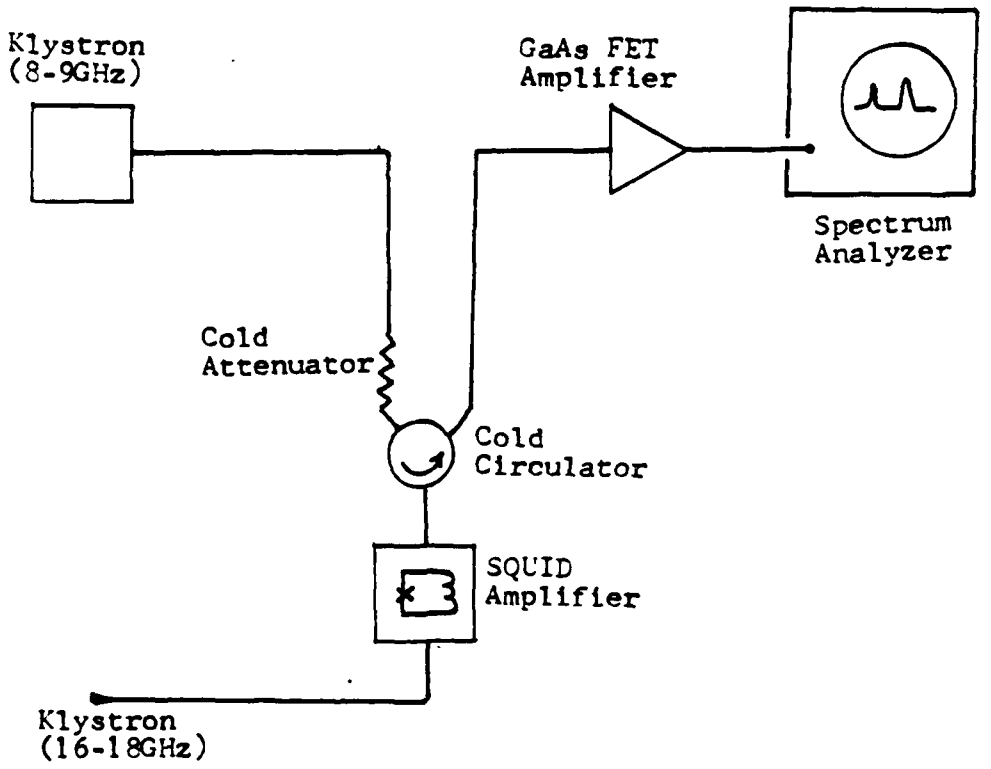

Figure 1. Block diagram of the microwave experimental arrangement for measuring the SQUID parametric amplifier performance.

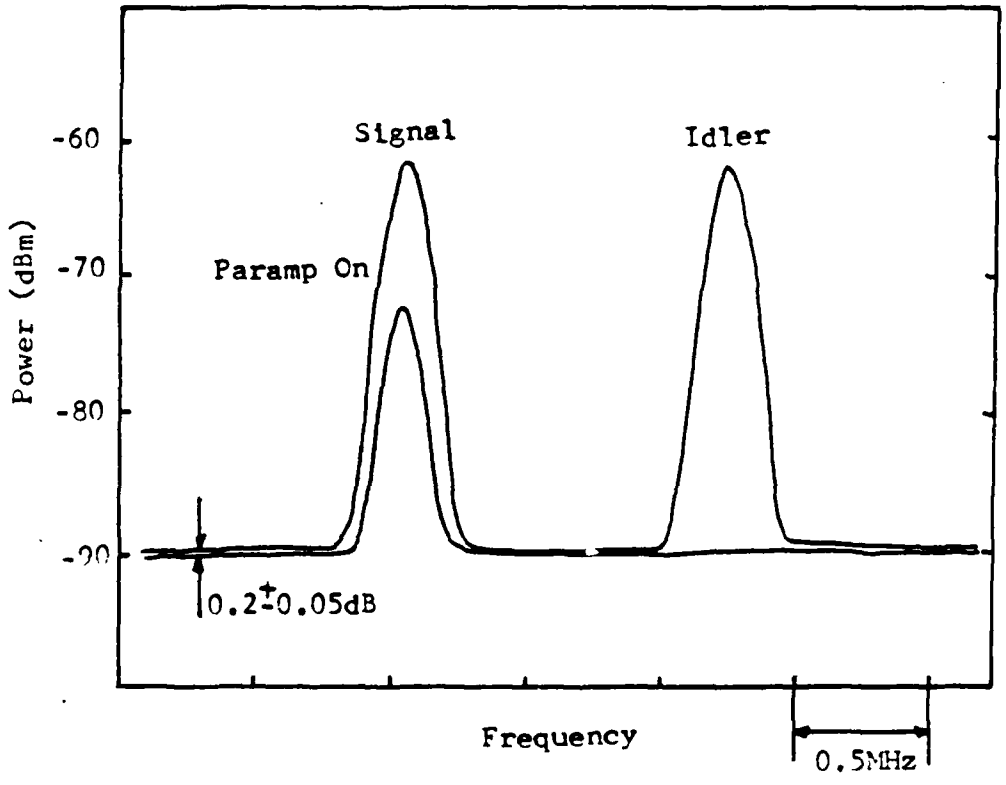

Figure 2. Typical small signal amplifier spectral response as recorded from the spectrum analyzer.

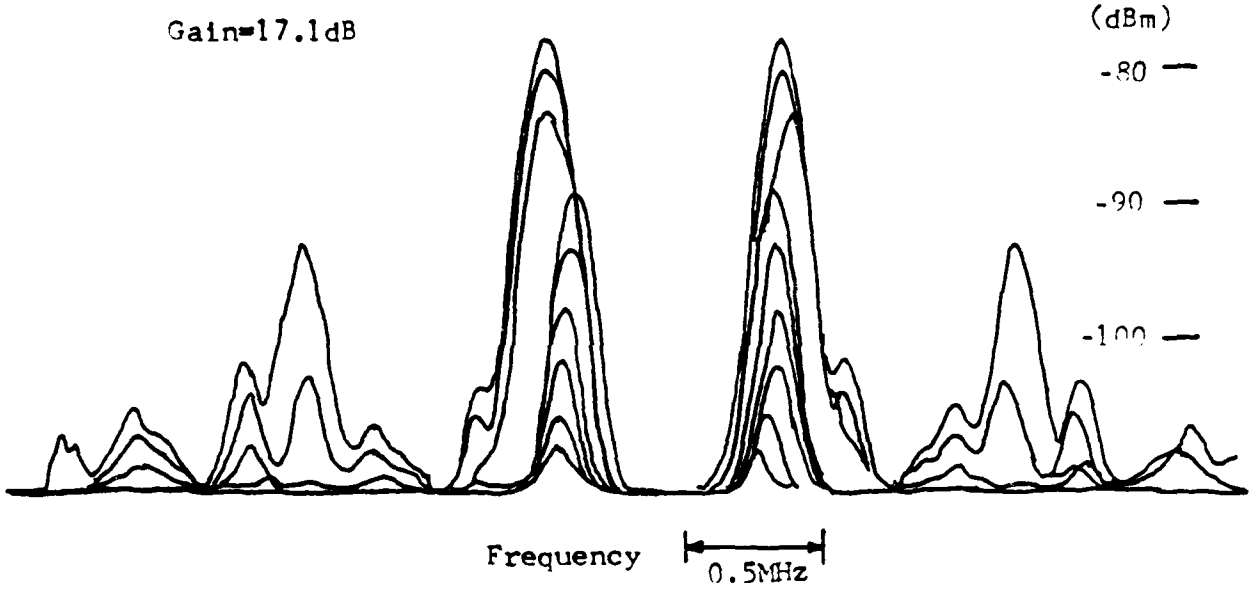

Figure 3. High gain spectral response of the SQUID amplifier as a function of signal power. Successive curves were recorded for 5 dB increases in the signal.

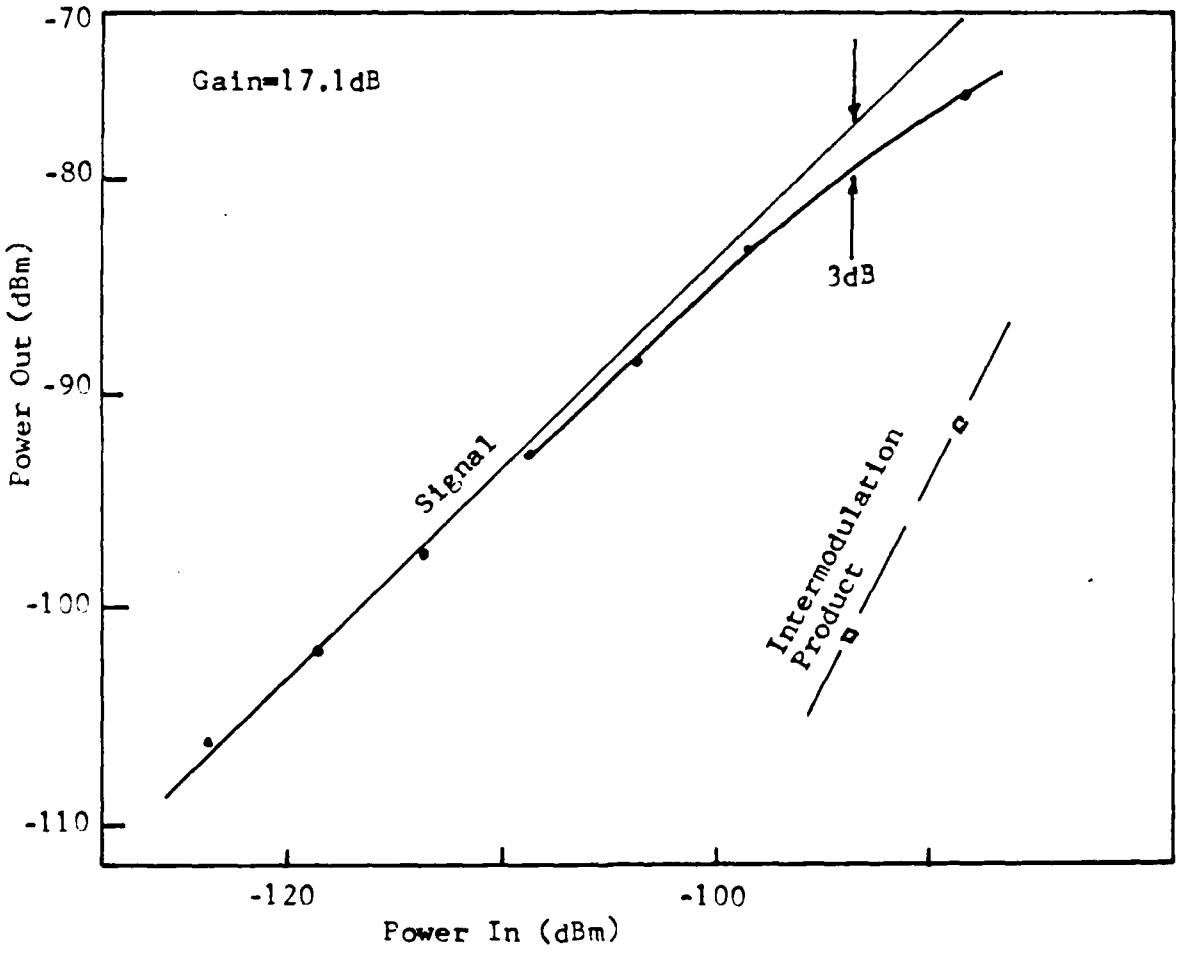

Figure 4. Measured output power versus the input power for the signal and intermodulation product as shown in Fig. 3.

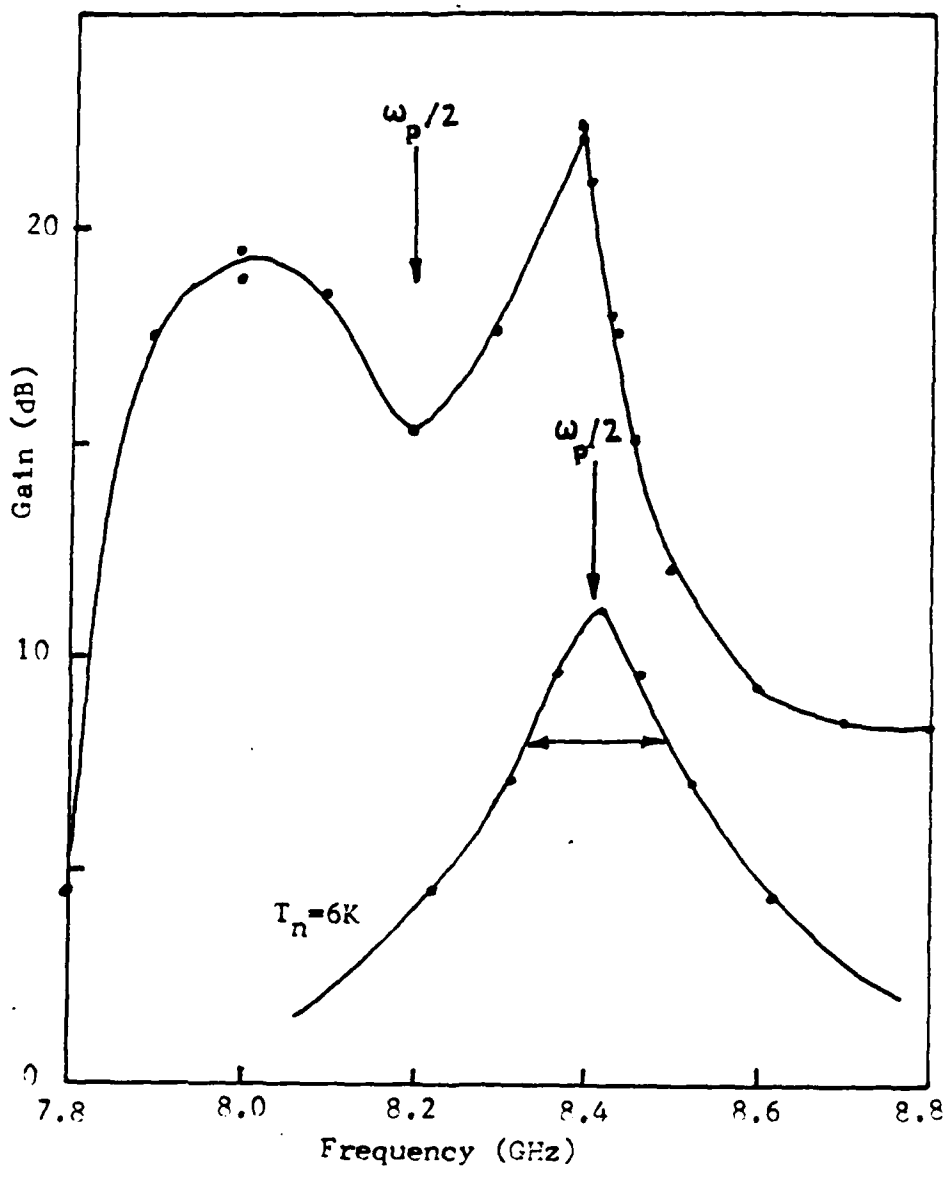

Figure 5. Measured spectral response of the SQUID parametric amplifier as a function of signal frequency for both a high gain and low gain case. The pump subharmonic frequency is shown by the arrows on the graph.

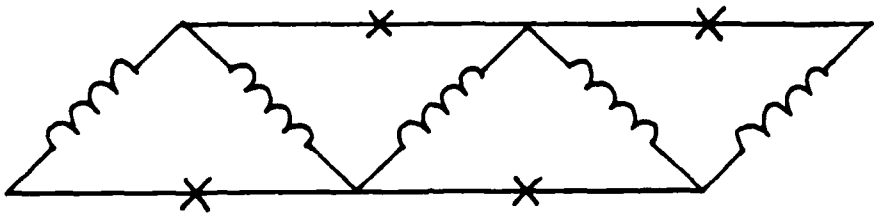

Equivalent Circuit

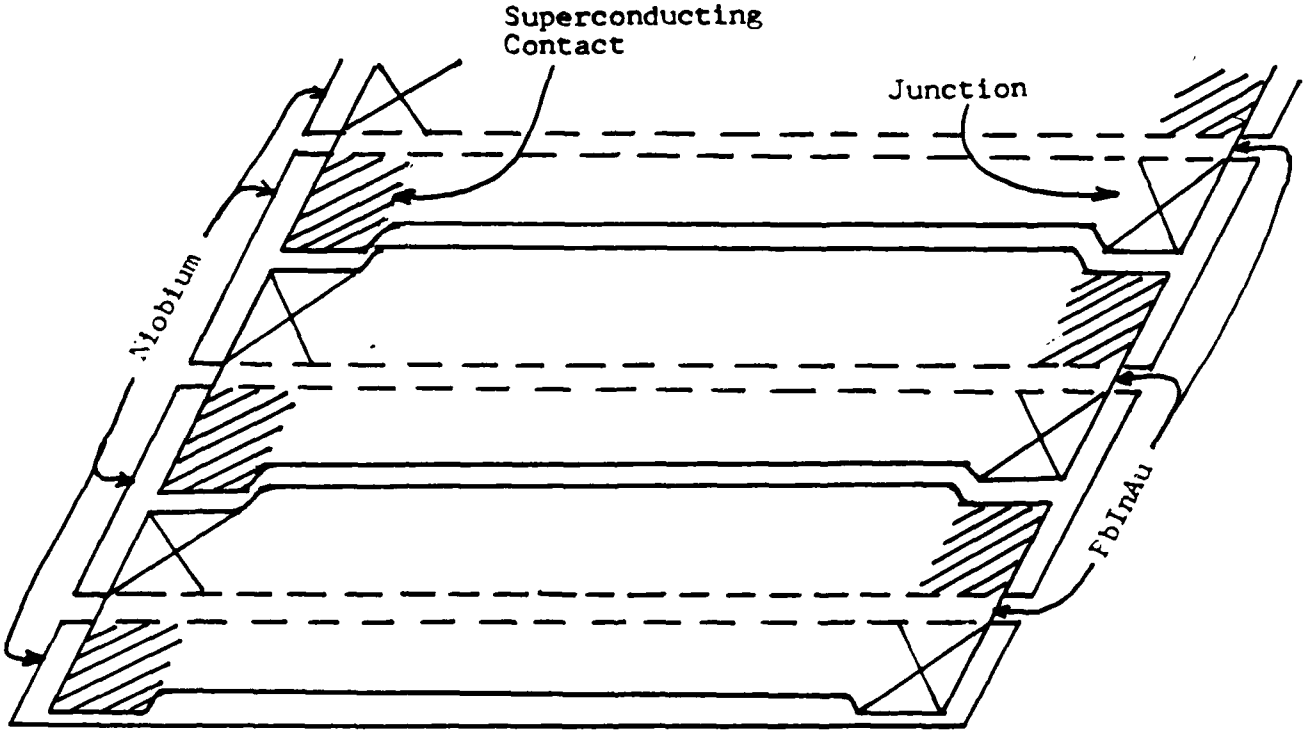

Figure 6. Schematic drawing of the geometry of the SQUID paramp array (not to scale).

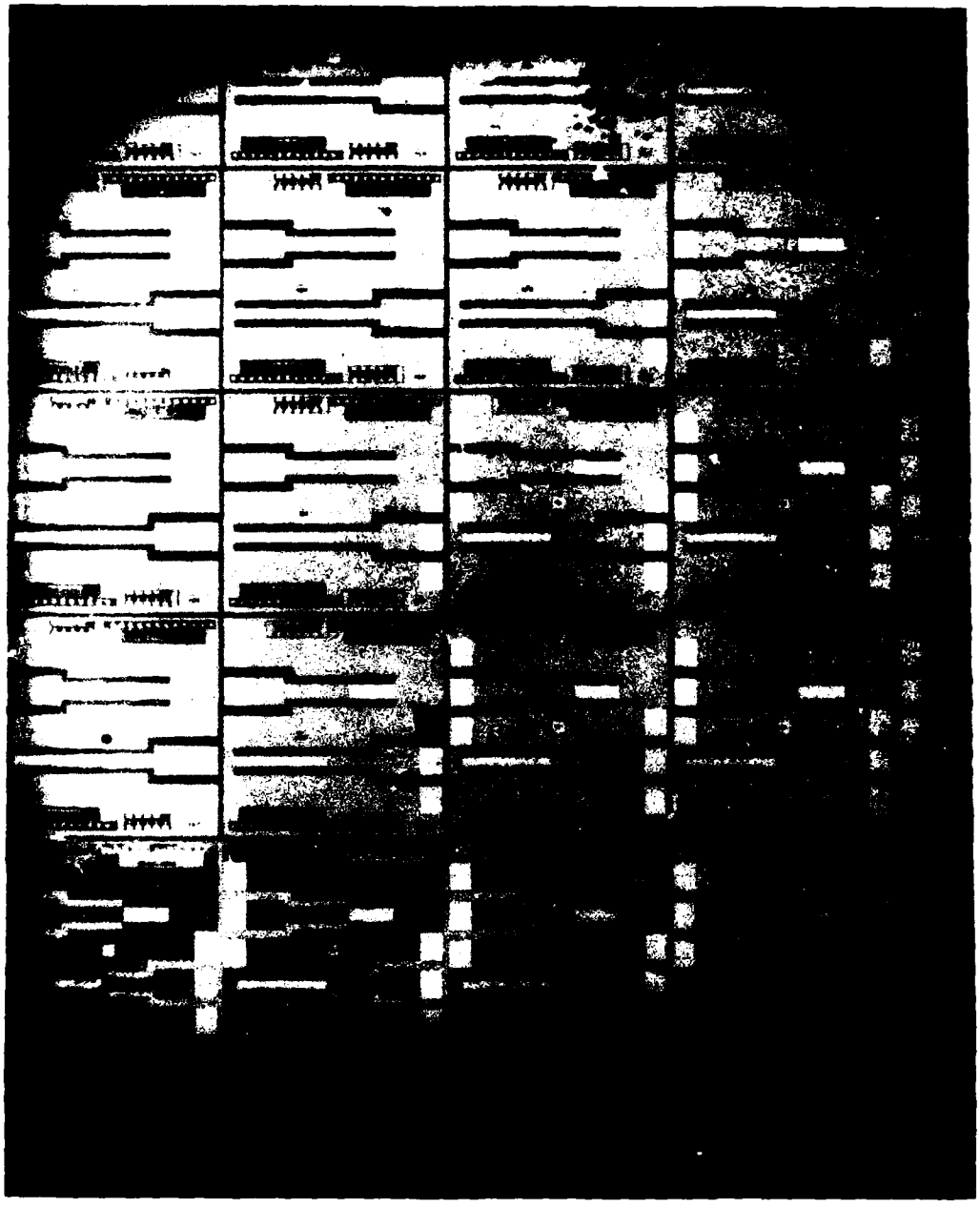

Figure 7. Photograph of a fabricated paramp array two inch silicon wafer.

Figure 8. Photograph of the SQUID paramp array chip showing the two different size arrays.

8. DISTRIBUTION LIST FOR TECHNICAL REPORTS
CONTRACT NO. N00014-81-C-2495

Dr. Martin N. Nisenoff, Code 6854 COTR Contract No. N00014-81-C-2495 Naval Research Laboratory 4555 Overlook Avenue, S.W. Washington, DC 20375	50
Administrative Contracting Officer Naval Research Laboratory 4555 Overlook Avenue, S.W. Washington, DC 20375 Ref: Contract No. N00014-81-C-2495	1
Director Naval Research Laboratory 4555 Overlook Avenue, S.W. Washington, DC 20375 Attn: Code 2627	6
Defense Technical Information Center Building 5 Cameron Station Alexandria, VA 22314	12
Mr. Edgar A. Edelsack Code 414 Office of Naval Research 800 North Quincy Street Arlington,, VA 22217	1
Dr. Fernand D. Bedard Department of Defense R03 Fort Meade, MD 20755	1
Dr. Nancy D. Welker Department of Defense R03 Fort Meade, MD 20755	1

Mr. Max N. Yoder 1
Code 414
Office of Naval Research
800 North Quincy Street
Arlington, VA 22217

Dr. James E. Zimmerman 1
Mail Stop 2137
National Bureau of Standards
325 S. Broadway
Boulder, CO 80302

Dr. Clark A. Hamilton 1
Room 2137
National Bureau of Standards
325 S. Broadway
Boulder, CO 80302

Mr. Ernest Stern 1
MIT-P-327
Lincoln Laboratory
P.O. Box 73
Lexington, MA 02173

Dr. Ted Van Duzer 1
Dept. of Electrical Engineering and Computer Science
University of California
Berkeley, CA 94270

TRW Documents Section 1
Technical Information Center (TIC)
Building S, Room 1930
One Space Park
Redondo Beach, CA 90278

APPENDIX 1.

LOW NOISE MICROWAVE PARAMETRIC AMPLIFIER* A. D. Smith, R. D. Sandell, J. F. Burch, and A. H. Silver, TRW Space & Technology Group - We report the lowest noise temperature of any microwave amplifier except the maser. This amplifier is a nearly degenerate superconducting parametric amplifier at X-band consisting of a low-β, thin film, single junction SQUID, a monolithic 50 Ω to 1 Ω impedance matching network, and a cooled circulator. $Nb/Nb_2O_5/PbBi$ junctions were incorporated into Nb and lead-indium circuitry on 1 x 2 cm silicon chips. The SQUID was phase-biased near $\pi/2$ and driven by an external pump at approximately twice the operating frequency. The self-resonance arising from the SQUID inductance and junction capacitance was set near the operating frequency of 8.2 GHz, The SQUID was designed with a damping parameter (inverse Q) of 0.3, an inductance of 5 pH, and junction current density of 9 A/cm^2. The operating characteristics were dependent on the pump amplitude, the SQUID phase bias, and the SQUID β. For small values of $\beta \approx 1$, the maximum gain in both the signal and idler channels was ≈ 10 dB, the single-sideband noise temperature was 6 K within an uncertainty of (+15 to -7)K, and the bandwidth was ≈ 250 MHz. For higher β SQUIDs, the maximum gain increased near 30 dB with increased noise. Parametric oscillations were observed near the pump subharmonic for higher gain. Comparison of the measurements with theory, design of a high power array amplifier, and expected frequency dependence will be presented.

*Supported by the Naval Research Laboratory Contract No. N00014-81-C-2495

1. Category 8.
2. A. H. Silver, R1/2170, TRW Space & Technology Group One Space Park, Redondo Beach, CA 90278; (213) 535-2500.
3. A. D. Smith, R. D. Sandell, and A. H. Silver.
4. No preference.

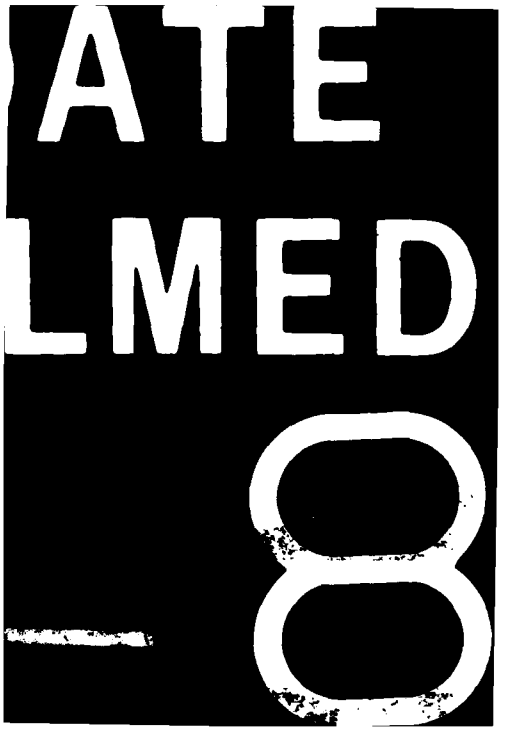
ATE
LMED
8